

Mesoscopic spin-orbit effect in the semiconductor nanostructure electron g factor

M. A. Toloza Sandoval,¹ A. Ferreira da Silva,¹ E. A. de Andrada e Silva,² and G. C. La Rocca³

¹*Instituto de Física, Universidade Federal da Bahia 40210-340, Salvador, Bahia, Brazil*

²*Instituto Nacional de Pesquisas Espaciais, C.P. 515, 12201-970 São José dos Campos, São Paulo, Brazil*

³*Scuola Normale Superiore and CNISM, Piazza dei Cavalieri 7, I-56126 Pisa, Italy*

(Received 16 March 2012; published 5 November 2012)

The renormalization of the electron g factor by the confining potential in semiconductor nanostructures is considered. A new effective $\mathbf{k} \cdot \mathbf{p}$ Hamiltonian for the electronic states in III–V semiconductor nanostructures in the presence of an external magnetic field is introduced. The mesoscopic spin-orbit (Rashba type) and Zeeman interactions are taken into account on an equal footing. It is then solved analytically for the electron effective g factor in symmetric quantum wells (g_{QW}^*). Comparison with different spin quantum beat measurements in GaAs and InGaAs structures demonstrates the accuracy and utility of the theory. The quantum size effects in g_{QW}^* are easily understood and its anisotropy Δg_{QW}^* (i.e., the difference between the in-plane and perpendicular configurations) is shown to be given by a mesoscopic spin-orbit effect having the same origin as the Rashba one.

DOI: 10.1103/PhysRevB.86.195302

PACS number(s): 73.21.Fg, 78.67.—n

I. INTRODUCTION

The Landé g factor is a fundamental physical quantity that determines the spin splitting of the electronic states in response to an external magnetic field, known as Zeeman effect. For charge and spin carriers in semiconductors, the g factor is renormalized from the bare value 2 by band structure effects and is referred to as the effective g factor (g^*), in analogy with the effective mass (m^*). In semiconductor nanostructures g^* is further renormalized by the confining mesoscopic potential and can therefore be tuned. However, despite its great scientific and technological interest, such effect is still not well understood and, here, a simple solution is presented.

Among the III–V semiconductors, the electron g^* varies, for example, from ~ -0.5 in GaAs to ~ -50 in InSb. Such variation is well explained by the celebrated Roth $\mathbf{k} \cdot \mathbf{p}$ formula

$$g^* = 2 \left(1 - \frac{m_e}{m^*} \frac{\Delta}{3E_g + 2\Delta} \right), \quad (1)$$

(m^*/m_e being the electron effective mass in units of the free-electron mass, Δ the valence-band SO splitting, and E_g the fundamental energy gap). This expression was derived by Roth, Lax, and Zwerdling¹ with second-order perturbation theory, including only the interaction with the valence-band, and corresponds to the exact Kane model solution at the conduction band edge.²

More recently, in semiconductor spintronics, there is great interest in the electron g -factor control or tuning for spin manipulation, which can be achieved with quantum confinement effects in nanostructures. The electron effective g factor in III–V QWs (g_{QW}^*) has been then much investigated both experimentally^{3–11} and theoretically,^{12–19} and the overall g_{QW}^* variation with the QW width L is well established. However, for example, the well-width dependence of the basic anisotropy Δg_{QW}^* (the difference between in-plane and perpendicular g_{QW}^* ; see Fig. 1) is still not well understood.

Experimentally, g_{QW}^* has been studied with the coincidence method in tilted magnetic fields,^{3,10} with spin flip Raman scattering,⁷ and with spin quantum beats,^{5,8,9} which allowed detailed measurements of Δg_{QW}^* as a function of L . Such anisotropy was predicted by Ivchenko and Kiselev¹² with an

envelope-function theory based on the Kane model. The theory has been used to study the electron g^* in QWs of GaAs,^{5,8,9,12} strained InGaAs,⁹ CdTe,^{7,11,15} GaN,¹⁵ and with bias,¹³ and has also been extended to quantum wires and dots.¹⁴ However, its numerical results do not fit very well the quantum beat data for Δg_{QW}^* in GaAs^{8,9} and InGaAs⁹ QWs. The physical picture for the anisotropy is also not very transparent; it is ascribed to the difference between the light and heavy hole effective masses, which are not well described by the Kane model. Most importantly, it is also still not clear what is the relation between g_{QW}^* and the Rashba SO coupling, for which different indications exist.^{10,20,21} Finally, despite representing the most natural QW extension of the analytical bulk result in Eq. (1),²² the use of the theory in Ref. 12 requires instead nontrivial numerical calculations.

Here we present an alternative solution for g_{QW}^* with none of these problems. A simple and accurate expression is derived that shows that the anisotropy Δg_{QW}^* is given by a mesoscopic SO term as the Rashba one. Based on standard envelope function theory,^{23,24} we first derive an effective Hamiltonian for a single electron in an undoped QW in the presence of an external magnetic field, where the Rashba and the effective Zeeman couplings appear on an equal footing. Then with first-order perturbation theory we obtain our expressions for $g_{\text{QW}}^*(L)$ and $\Delta g_{\text{QW}}^*(L)$.

II. EFFECTIVE HAMILTONIAN

We first consider the magnetic field in the QW plane, along y , i.e., $\vec{B} = (0, B, 0)$, and use the Landau gauge with $\vec{A} = (zB, 0, 0)$. Then in the $8 \times 8 \mathbf{k} \cdot \mathbf{p}$ Hamiltonian we set $k_y = 0$ (i.e., consider the bottom of the subband), add the bare Zeeman interaction, make the fundamental substitution $\vec{k} \rightarrow \vec{k} + \frac{e}{\hbar} \vec{A}$ ($-e$ being the electron charge), and following Ref. 24, perform the projection into the conduction band. Finally, by writing the conduction band envelope function as $F = f_{k_x}(z)e^{ik_x x}$,²⁵ we obtain

$$H_{\text{eff}} = H_0 + H_R + H_Z,$$

i.e., an effective Hamiltonian for electrons in a QW with in-plane magnetic field given by the sum of three terms: a spin-

independent term,

$$H_0 = -\frac{\hbar^2}{2} \frac{d}{dz} \frac{1}{m^*(z, \varepsilon)} \frac{d}{dz} + \frac{\hbar^2 (k_x + z/l^2)^2}{2m^*(z, \varepsilon)} + E_c(z), \quad (2)$$

$l = \sqrt{\hbar/eB}$ being the magnetic length; a Rashba SO coupling term,

$$H_R = -\sigma_y k_x \frac{d}{dz} \beta(z, \varepsilon), \quad (3)$$

$\frac{\hbar}{2} \sigma_y$ being the y component of the spin operator; and an effective Zeeman term,

$$H_Z = \frac{1}{2} \left[g_{\text{bulk}}^*(z, \varepsilon) - \frac{4m_e}{\hbar^2} z \frac{d}{dz} \beta(z, \varepsilon) \right] \mu_0 \sigma_y B, \quad (4)$$

$\mu_0 = e\hbar/2m_e$ being the Bohr magneton and

$$g_{\text{bulk}}^*(z, \varepsilon) = 2 - \frac{4m_e}{\hbar^2} \beta(z, \varepsilon) + \delta g_{\text{rem}}. \quad (5)$$

In the above equation, δg_{rem} represents the correction due to all the remote bands not included in the Kane model.²⁶ The effective mass and the SO β parameter are given by

$$\frac{1}{m^*(z, \varepsilon)} = \frac{P^2}{\hbar^2} \left[\frac{2}{\varepsilon - E_v(z)} + \frac{1}{\varepsilon - E_v(z) + \Delta(z)} \right], \quad (6)$$

and

$$\beta(z, \varepsilon) = \frac{P^2}{2} \left[\frac{1}{\varepsilon - E_v(z)} - \frac{1}{\varepsilon - E_v(z) + \Delta(z)} \right]; \quad (7)$$

P being the momentum matrix element. Note that by measuring the electron energy from the bottom of conduction band of the well material, one has $E_c = 0$ in the well and $E_c = v_0 (= Q_c \Delta E_g, Q_c$ being the conduction band offset) in the barrier; while $E_v = -E_g^w$ and $-E_g^b + v_0$ in the well and in the barrier, respectively.

First, it is easy to check that the above obtained H_{eff} reduces exactly to well-known effective Hamiltonians in three important limits: (1) zero magnetic field^{24,27}—the Kane QW effective Hamiltonian, with Rashba SO coupling, is recovered, note that for $B = 0$ the quantum number k_x , which gives the center of the cyclotron orbit $z_0 = -l^2 k_x$, turns into the usual in-plane (or parallel) electron wave-vector, and the usual Rashba term is recovered. (2) No SO interaction ($\Delta = 0$)²⁵— H_{eff} for the in-plane QW Landau levels is recovered; and (3) the bulk limit²—the Kane nonparabolic bulk conduction band H_{eff} with the effective Zeeman interaction is recovered. Our H_{eff} generalizes then these models and allows the study of the interplay between the Rashba and Zeeman effects in QWs, with an accurate multiband description of the bulk bands around the semiconductor fundamental gap, without requiring elaborate numerical calculations.

III. QW g FACTOR

The Zeeman term [Eq. (4)] is seen to be made of a bulk plus an interface contribution.²⁸ Despite the same coupling parameter $\alpha_R = \frac{d}{dz} \beta$,²⁴ this g -factor interface contribution has, however, different behavior than H_R . For example, while there is Rashba spin splitting only in asymmetric QWs (in symmetric QWs the contributions of the two interfaces cancel out), in the effective g factor the contributions of the two interfaces have

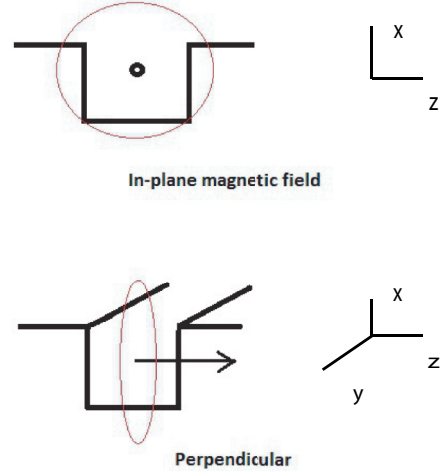


FIG. 1. (Color online) Illustration of the in-plane and perpendicular magnetic field configurations in a QW with growth direction along z . The arrow indicates the direction of the field and is seen from the top in the upper panel. The corresponding *classical* (real space) cyclotron orbit is also sketched, illustrating the fact that an in-plane magnetic field drives the electrons across the QW interfaces contrary to the perpendicular configuration.

the same sign and are added together in both symmetric and asymmetric QWs. Since H_Z is already explicitly linear with B , the in-plane g_{QW}^* can then be obtained with the coefficient calculated at $B = 0$. In first-order perturbation theory it means:

$$g_{\text{QW}}^* = \langle f^{(0)} | g_{\text{bulk}}^*(z, \varepsilon_0) - \frac{4m_e}{\hbar^2} z \frac{d}{dz} \beta(z, \varepsilon_0) | f^{(0)} \rangle, \quad (8)$$

where the unperturbed problem $H_0(B = 0)f^{(0)} = \varepsilon_0 f^{(0)}$ corresponds to the Kane QW problem.²⁹

Considering now a symmetric QW with interfaces at $z = \pm L/2$ and recalling that β is a step function in z at the interfaces (where it changes from β_w to β_b), one finds

$$g_{\text{QW}}^* = \bar{g}_{\text{bulk}}^* + \frac{4m_e}{\hbar^2} \delta\beta L |f^{(0)}(L/2)|^2, \quad (9)$$

where $\delta\beta = \beta_w - \beta_b$ and $\bar{g}_{\text{bulk}}^* = g_w^* P_w + g_b^* P_b$ is the QW averaged bulk g factor, $P_i (= \int_i |f^{(0)}(z)|^2 dz)$ being the probability to find the electron in the region $i = \text{barrier or well}$, and we have used $|f^{(0)}(L/2)|^2 = |f^{(0)}(-L/2)|^2$. So we get a g_{QW}^* , which is given by the averaged bulk g^* plus an interface mesoscopic SO contribution, which goes to zero both for $L = 0$ and for L going to infinity. In these limits, Eq. (1) is recovered (except for δg_{rem}).

By rotating the magnetic-field to align it with the growth direction (i.e., $\vec{B} = B\hat{z}$), one restores the QW axial symmetry and the g -factor interface SO term goes to zero (similarly to the Rashba coupling when the parallel wave-vector goes to zero). One then obtains the perpendicular g_{QW}^* simply given by \bar{g}_{bulk}^* , and the anisotropy $\Delta g_{\text{QW}}^* = \frac{4m_e}{\hbar^2} \delta\beta L |f^{(0)}(L/2)|^2$, i.e., equal to the obtained g -factor interface SO contribution. This result provides a simple physical interpretation for the g_{QW}^* anisotropy. From the sketch in Fig. 1, it is indeed intuitively clear that only for in-plane fields the cyclotron orbit drives the electrons across the interfaces, so to feel the mesoscopic SO coupling there.

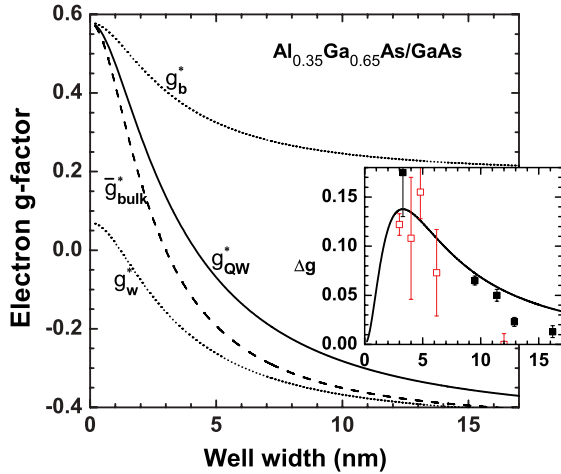


FIG. 2. (Color online) Calculated effective electron g factor as a function of the GaAs quantum well width. The inset compares the obtained anisotropy with the measurements in Refs. 8 (empty red symbols) and 9 (filled black symbols). The parameters being $m_w^* = 0.067 m_e$, $E_g^w = 1.52$ eV, $\Delta^w = 0.34$ eV, $\delta g_{\text{rem}}^w = -0.50$, $E_g^b = 1.94$ eV, $\Delta^b = 0.32$ eV, $\delta g_{\text{rem}}^b = 0.13$, and $v_0 = 0.277$ eV.

IV. EXAMPLES

As specific examples, we consider now the g factor in GaAs and InGaAs QWs and compare with quantum beat measurements. All one has to do is to calculate ε_0 and $f^{(0)}(z)$ as a function of L (see Appendix) and substitute them in Eqs. (5) and (9). Figures 2 and 3 show the results obtained for the electron g factor in lattice matched AlGaAs/GaAs and InP/InGaAs QWs.³⁰ Besides the in-plane $g_{\text{QW}}^*(L)$ [Eq. (9)], we plot also $g_w^*(\varepsilon_0)$, \bar{g}_{bulk}^* , and $g_b^*(\varepsilon_0)$. For $L = 0$, as expected, $g_{\text{QW}}^* = \bar{g}_{\text{bulk}}^* = g_b^*(v_0) = g_b^*$, while for large values of L , both g_{QW}^* and \bar{g}_{bulk}^* slowly tend to g_w^* . The anisotropy in the smaller gap InGaAs QW is larger due to the stronger SO coupling and leads to a corresponding larger range of well-widths in which

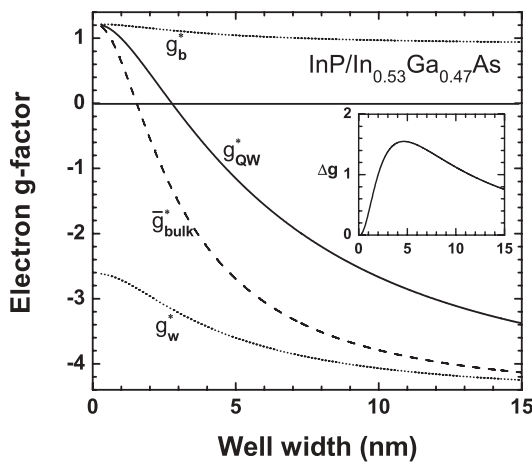


FIG. 3. As described in the legend of Fig. 2, obtained g_{QW}^* for lattice-matched InGaAs QWs. The parameters used are $m_w^* = 0.041 m_e$, $E_g^w = 0.813$ eV, $\Delta^w = 0.326$ eV, $\delta g_{\text{rem}}^w = -1.36$, $E_g^b = 1.424$ eV, $\Delta^b = 0.108$ eV, $\delta g_{\text{rem}}^b = 0.24$, and $v_0 = 0.244$.

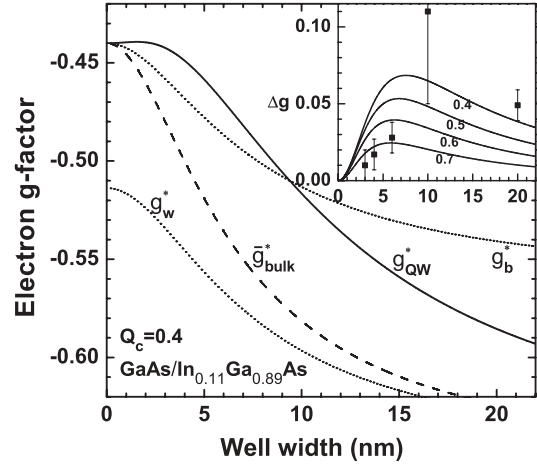


FIG. 4. Obtained effective electron g factor for strained InGaAs QWs as a function of the well width. The inset shows the calculated g -factor anisotropy for varying conduction band-offset Q_c together with the experimental results of Ref. 9. The parameters used are $m_w^* = 0.062 m_e$, $E_g^w = 1.394$ eV, $\Delta^w = 0.333$ eV, $\delta g_{\text{rem}}^w = -0.43$ for the InGaAs well and $E_g^b = 1.53$ eV, $\Delta^b = 0.34$ eV, $\delta g_{\text{rem}}^b = -0.50$ for the GaAs barrier.

the in-plane (g_{QW}^*) and perpendicular (\bar{g}_{bulk}^*) QW effective g factors have opposite signs.

It is interesting to note the following hierarchy of approximations to g_{QW}^* : first, $g_w^*[\varepsilon_0(L)]$, which considers and gives only the nonparabolicity correction to g_w^* ,² due to the QW zero-point energy; then, \bar{g}_{bulk}^* , which includes the barrier penetration effects and gives the perpendicular g_{QW}^* (including nonparabolicity corrections also in g_b^*), and finally, the in-plane g_{QW}^* , which includes also the SO interface contribution.

Another interesting example is the strained GaAs/InGaAs QWs. First, because for small In concentrations, g_w^* and g_b^* are similar and the interface contribution becomes then particularly important; and second, because Δg_{QW}^* in these QWs has been measured.⁹ Figure 4 shows that in these QWs the SO interface contribution plays indeed an important role, to the point that for $L \leq 10$ nm, $g_{\text{QW}}^* \geq g_b^*$ and presents a soft maximum near $L = 3$ nm. In the inset, the results for the anisotropy calculated with different conduction-band offsets (i.e., $Q_c = 0.4, 0.5, 0.6$, and 0.7) are compared with the experimental data. Considering also the uncertainties (not shown) in the sample In content and well width, the inset becomes an indication that the band offset in these QWs is closer to 0.4 than to 0.7, in accord to the last entries in this dispute.³¹

V. CONCLUSIONS

We have presented an envelope-function theory for the renormalization of the electron g factor by the confining mesoscopic potential in semiconductor nanostructures. The obtained results, in particular regarding the solution for the problem of the electron g factor in semiconductor QWs, give us enough ground to believe that the theory can be very useful in the nanostructure electron g factor tuning effort. It provides a simple analytical expression for $g_{\text{QW}}^*(L)$ [Eq. (9)], which applies to general III-V QWs and also an intuitive physical picture for the mesoscopic spin-orbit effect in these structures.

For instance, the well-known QW g -factor anisotropy is shown to be due to such mesoscopic spin-orbit (Rashba type) effect and is then simply explained.

A new effective Hamiltonian has been introduced for the calculation of the nanostructure electronic states in the presence of an external magnetic field; which can be used in the study of the electron g factor and of the interplay between Rashba and Zeeman interactions in asymmetric QWs, double-barrier structures, and superlattices as well. The mesoscopic spin-orbit (Rashba) and Zeeman effects are taken into account on an equal footing; and the good agreement with independent spin quantum beat measurements in GaAs and InGaAs QWs demonstrates the accuracy and potential utility of the theory.

ACKNOWLEDGMENTS

The authors thank the Brazilian agencies CNPq, FAPESP, CAPES, and FAPESB for financial support. E.A.A.S. is also thankful to the Scuola Normale Superiore di Pisa, for the kind hospitality during part of this work.

APPENDIX

In this Appendix, we give the solution used here for the energy and envelope function of an electron confined in a

square QW, described by the Kane model. It is an exact solution where the envelope function for the first subband is given by:

$$f^{(0)}(z) = \begin{cases} A_b e^{-k_b|z|} & , \quad |z| \geq L/2 \\ A_w \cos k_w z & , \quad |z| \leq L/2 \end{cases} \quad (\text{A1})$$

where $k_w = \sqrt{2m_w \varepsilon_0 / \hbar^2}$ and $k_b = \sqrt{2m_b(v_0 - \varepsilon_0) / \hbar^2}$ (v_0 being the QW barrier height, i.e., the interface conduction band offset). From the normalization and boundary conditions, one then obtains

$$A_b = \left\{ \frac{e^{-k_b L}}{k_b} \left[1 + \frac{k_b}{2k_w} \frac{\sin(k_w L) + k_w L}{\cos^2(k_w L/2)} \right] \right\}^{-1/2}, \quad (\text{A2})$$

$$A_w = A_b \frac{e^{-k_b L/2}}{\cos(k_w L/2)} \quad (\text{A3})$$

and that the subband energy ε_0 is given by the lowest solution of the following transcendental equation:

$$\tan(k_w L/2) = \sqrt{\frac{m_w}{m_b} \left(\frac{2m_w v_0}{\hbar^2 k_w^2} - 1 \right)}. \quad (\text{A4})$$

Recall that the effective masses m_w and m_b are energy dependent, i.e., $m_{w,b} = m_{w,b}(\varepsilon_0)$ as given by Eq. (6).

¹L. M. Roth, B. Lax, and S. Zwerdling, *Phys. Rev.* **114**, 90 (1959).

²N. Kim, G. C. La Rocca, and S. Rodriguez, *Phys. Rev. B* **40**, 3001 (1989).

³T. P. Smith III and F. F. Fang, *Phys. Rev. B* **35**, 7729 (1987).

⁴M. J. Snelling, G. P. Flinn, A. S. Plaut, R. T. Harley, A. C. Tropper, R. Eccleston, and C. C. Phillips, *Phys. Rev. B* **44**, 11345 (1991).

⁵R. M. Hannak, M. Oestreich, A. P. Heberle, W. W. Rühle, and K. Köhler, *Solid State Commun.* **93**, 313 (1995).

⁶Q. X. Zhao, M. Oestreich, and N. Magnea, *Appl. Phys. Lett.* **69**, 3704 (1996).

⁷A. A. Sirenko, T. Ruf, M. Cardona, D. R. Yakovlev, W. Ossau, A. Waag, and G. Landwehr, *Phys. Rev. B* **56**, 2114 (1997).

⁸P. Le Jeune, D. Robart, X. Marie, T. Amand, M. Brosseau, J. Barrau, and V. Kalevcih, *Semicond. Sci. Technol.* **12**, 380 (1997).

⁹A. Malinowski and R. T. Harley, *Phys. Rev. B* **62**, 2051 (2000).

¹⁰X. C. Zhang, K. Ortner, A. Pfeuffer-Jeschke, C. R. Becker, and G. Landwehr, *Phys. Rev. B* **69**, 115340 (2004).

¹¹S. Tomimoto, S. Nozawa, Y. Terai, S. Kuroda, K. Takita, and Y. Masumoto, *Phys. Rev. B* **81**, 125313 (2010).

¹²E. L. Ivchenko and A. A. Kiselev, *Fiz. Tekh. Poluprovodn. (S.-Peterburg)* **26**, 1471 (1992) [*Sov. Phys. Semicond.* **26**, 827 (1992)].

¹³E. Ivchenko, A. Kiselev, and M. Willander, *Solid State Commun.* **102**, 375 (1997).

¹⁴A. A. Kiselev, E. L. Ivchenko, and U. Rössler, *Phys. Rev. B* **58**, 16353 (1998).

¹⁵A. A. Kiselev, K. W. Kim, and E. L. Ivchenko, *Phys. Status Solidi B* **215**, 235 (1999).

¹⁶R. Kotlyar, T. L. Reinecke, M. Bayer, and A. Forchel, *Phys. Rev. B* **63**, 085310 (2001).

¹⁷M. de Dios-Leyva, E. Reyes-Gómez, C. A. Perdomo-Leiva, and L. E. Oliveira, *Phys. Rev. B* **73**, 085316 (2006).

¹⁸P. Pfeffer and W. Zawadzki, *Phys. Rev. B* **74**, 233303 (2006).

¹⁹A. Bruno-Alfonso, F. E. López, N. Raigoza, and E. Reyes-Gómez, *Eur. Phys. J. B* **74**, 319 (2010).

²⁰Z. Wilamowski, W. Jantsch, H. Malissa, and U. Rössler, *Phys. Rev. B* **66**, 195315 (2002).

²¹J. S. de Sousa, H. Detz, P. Klang, E. Gornik, G. Strasser, and J. Smoliner, *Appl. Phys. Lett.* **99**, 152107 (2011).

²²Note that g_{QW}^* has been studied also with the Ogg-McCombe Hamiltonian^{17,19} and with $14 \times 14 \mathbf{k} \cdot \mathbf{p}$ model.¹⁸

²³E. A. de Andrada e Silva, G. C. La Rocca, and F. Bassani, *Phys. Rev. B* **50**, 8523 (1994).

²⁴E. A. de Andrada e Silva, G. C. La Rocca, and F. Bassani, *Phys. Rev. B* **55**, 16293 (1997).

²⁵G. Brozak, E. A. de Andrada e Silva, L. J. Sham, F. DeRosa, P. Miceli, S. A. Schwarz, J. P. Harbison, L. T. Florez, and S. J. Allen, Jr., *Phys. Rev. Lett.* **64**, 471 (1990).

²⁶Assuming that the Kane model gives a perfect description of the 8 bands it does include, δg_{rem} is then given by the difference between the g factor measured experimentally in the bulk and that given by the Roth formula of Eq. (1).

²⁷L. G. Gerchikov and A. V. Subashiev, *Fiz. Tekh. Poluprovodn. (S.-Peterburg)* **26**, 131 (1992) [*Sov. Phys. Semicond.* **26**, 73 (1992)].

²⁸Note that in a flat band QW, $\alpha_R = \frac{d}{dz} \beta$ is different than zero only at the interfaces.

²⁹Note that for $B = 0$, $f_{k_x}^{(0)} = f^{(0)}$, i.e., does not depend on the center of the orbit; and that we consider the bottom of the subband corresponding to $k_x = 0$.

³⁰The values of the parameters used, indicated in the figure captions, are as in Refs. 23 and 24, except for the experimental bulk g factors, which are from Refs. 8 and 9 [see also H. Kosada *et al.*, *Electron. Lett.* **37**, 464 (2001)].

³¹W. S. Chi and Y. S. Huang, *Semicond. Sci. Technol.* **10**, 127 (1995).